Performance Analysis of a Variable Conductance Heat Pipe

A Senior Project

presented to

the Faculty of the Aerospace Department

California Polytechnic State University, San Luis Obispo

In Partial Fulfillment

of the Requirements for the

Bachelor of Science Degree in Aerospace Engineering

by

Herron Arreola

October, 2011

Acknowledgements

I would like to thank my advisor, Dave Esposto, for always pointing me in the right direction and asking the right questions, Dr. Tina Jameson for taking time to answer questions and loaning me the necessary equipment for the experiment, David Knapp for locating and ordering equipment as well as setting up the lab time, Daniel Barath for machining the cooling box, helping with the design of the experiment and for being there during the experiment and my girlfriend, Patricia Gonzalez, for supporting me every step of the way.

Performance Analysis of a Variable Conductance Heat Pipe

Herron Arreola*
California Polytechnic State University, San Luis Obispo, California 93407

This report examines the analysis of a donated Boeing variable conductance heat pipe with unknown performance characteristics. These characteristics were found through experimental means by utilizing 14 thermocouples attached to various locations on the heat pipe, the heaters and to the insulation. Although the maximum axial heat transport capability could not be determined due to the limited number of strip heaters available, the maximum radial heat flux capability of the heat pipe was found to be 2.46 W/in^2. The experiment also revealed that increasing the input power decreased the burn out inclination angle and that using a coolant with a lower temperature (ice-water) decreased the wall temperatures of the pipe but not the performance. The active feedback control was also analyzed by attaching a patch heater to the reservoir and increasing the input power from 1 W to 8 W. The feedback system provided temperature control at the evaporator from 45 °C to 74 °C with a 4 °C accuracy while a constant 50 Watt input power was maintained at the strip heaters. The analysis was useful in determining the performance trends of the heat pipe through experimental means and provided the type of information that could verify design predictions or performance claims.

Nomenclature

A	=	Area	in^2
P	=	Power	W
R	=	Resistance	Ω
T	=	Temperature	K
V	=	Voltage	V
Q	=	Heat Flow	W
c	=	Specific Heat	J/kg°C
$\dot{m}$	=	Flow Rate	kg/s
q	=	Heat Flux	W/in^2

Subscripts

c	=	Cold (cooling box inflow)
h	=	Hot (cooling box outflow)
in	=	In
ins	=	Insulation
l	=	Lower
$loss$	=	Losses
out	=	Out
p	=	Constant Pressure
r	=	Radial
sup	=	Supplied
u	=	Upper

* Undergraduate Student, Aerospace Engineering Department, 1 Grand Ave, San Luis Obispo, CA 93407

I. Introduction

The basic idea of the heat pipe has been around for many years but has undergone many changes to best suit its application. The Perkins Tube[1] was introduced by the Perkins family during the mid to late 1800's and was an early form of a heat pipe known as a thermosyphon. Thermosyphons use gravity instead of a wick to get the liquid back to the evaporator. Unfortunately, this required the placement of the evaporator to be below the condenser. Figure 1[1] illustrates the Perkins Boiler, one of the earliest applications of the thermosyphon. The furnace below heats the water in the wickless tube, the water evaporates and the resulting vapor travels upwards, the vapor condenses as it heats the water in the boiler and the liquid in the tube travels back down assisted by gravity to repeat the process. Other uses were made of the thermosyphons such as baker's ovens and radiators each having their own limitations.

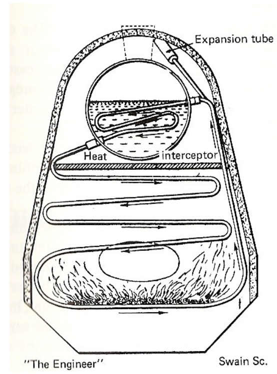

Figure 1. Perkins Boiler.

The concept of the heat pipe was not patented until 1944 when R.S. Gaugler[1] of the General Motor Corporation sought a method to move heat for a refrigeration unit where the evaporative section was above the condenser. He proposed a capillary structure to move the liquid from the condenser to the evaporator and suggested a sintered iron wick. Gaugler's heat pipe was never developed but the idea remained until 1962 when L. Trefethen[2] began to look at the possibilities of including this technology in the space program. By 1963, G.M. Grover filed a patent on behalf of the United States Atomic Energy Commission describing the term 'heat pipe' and included a theoretical analysis as well as experimental results for a stainless steel heat pipe utilizing a wire mesh wick and a sodium working fluid[1]. Research began at Los Alamos Laboratory in New Mexico headed by Grover where he built several prototypes. The work of T.P. Cotter[1], also working at Los Alamos, led to a well-developed theory of heat pipes and following his first publication in 1965 on heat pipe analysis, research programs also started in the U.K. and Italy.

Figure 2[1] illustrates the process of moving heat from the condenser to the evaporator in the heat pipe. The heat enters the evaporator causing the working fluid to vaporize. This vapor travels up the center of the pipe to the condenser section where it cools and changes from vapor to liquid. The liquid attaches to the wick and travels back to the evaporator through capillary action. The pressure caused by the capillary action (P_c) must be greater than the total pressures drop in the pipe. The total pressure drop is the pressure needed to move the vapor from the evaporator to the condenser (P_l), the pressure drop needed to move the liquid back to the evaporator (P_v) and the gravitational head (P_g)[1]. Throughout the development of the heat pipe various wick structures have been researched and continue to be experimented with in order to obtain larger capillary pumping action.

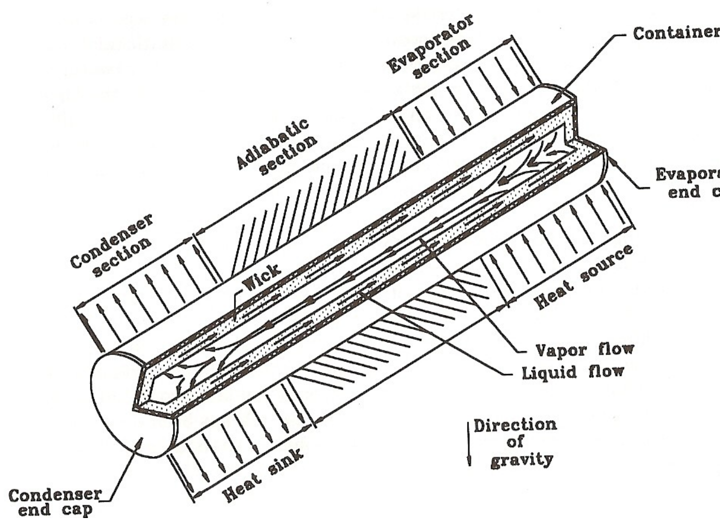

Figure 2. Constant conductance heat pipe schematic.

The first test of a heat pipe in space was launched in 1967[1]. The heat pipe had water as the working fluid with a stainless steel body and it performed as expected. The first actual use of heat pipes in space followed later that year

and they were utilized for thermal control on a GEOS-B satellite. The heat pipes were made from 6061 T-6 Aluminum alloy, utilized a 120 mesh aluminum wick and Freon 11 as the working fluid. The thermal system on the satellite with the heat pipes was found to be working better than a similar satellite that did not have heat pipes.

The research and development of the heat pipe brought with it many specialized applications such as rotating heat pipes, flexible heat pipes and flat plate heat pipes but it wasn't until the development of the variable conductance heat pipe (VCHP) that the true potential of their use in thermal control was realized. The VCHP allowed for a near-constant temperature control of components on spacecraft. Figure 3[2] displays a partially active and fully active VCHP. When less heat is introduced into the evaporator, less pressure is produced by the vapor. Because the pipe is a closed system, the gas in the reservoir expands to equalize the pressure. The expansion of the non-condensable gas blocks all or some of the condenser section and maintains the temperature at the evaporator. This form of passive thermal control can be varied by the type of working gas in the heat pipe. An active VCHP employs a heater on the reservoir with a feedback control system connected to a temperature sensor on the component. As the temperature on the component begins to drop, the feedback system provides power to the heater on the reservoir causing the non-condensable gas to expand and block the condenser. The active VCHP can control the temperature with much more precision but becomes a little more complex than the passive system. This report examines the performance of a VCHP and the precision of temperature control with an active system.

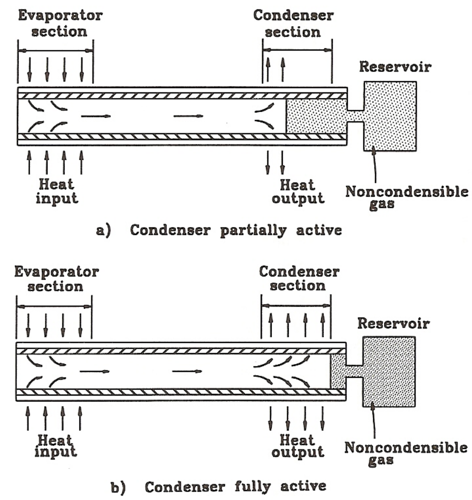

Figure 3. Variable conductance heat pipe with: a) Partially open condenser. b)Fully open condenser.

II. Apparatus and Procedure

Apparatus

Testing the VCHP required a set-up, shown in Fig. 4, which could measure temperatures, input heat, remove

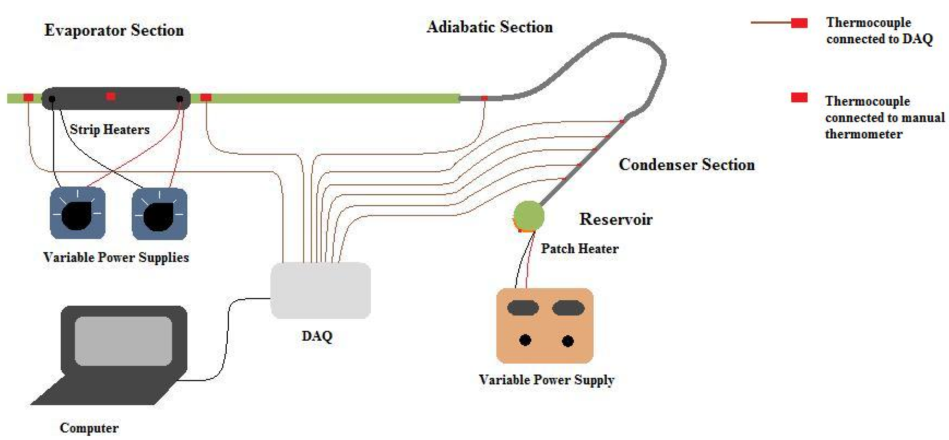

Figure 4. The experiment set-up as seen from the top view.

heat and trap heat in the system while inclining the oddly shaped heat pipe to the desired angles with accuracy. In order to measure the temperatures, eight type K thermocouples (shown in red) were placed along the heat pipe; two in the evaporator section, one in the adiabatic section and five along the condenser section.

Figure 5 displays the placement of the thermocouples attached directly to the heat pipe or the heaters. As can be seen in the figure, there were two thermocouples attached to the evaporator section (green), one on the adiabatic

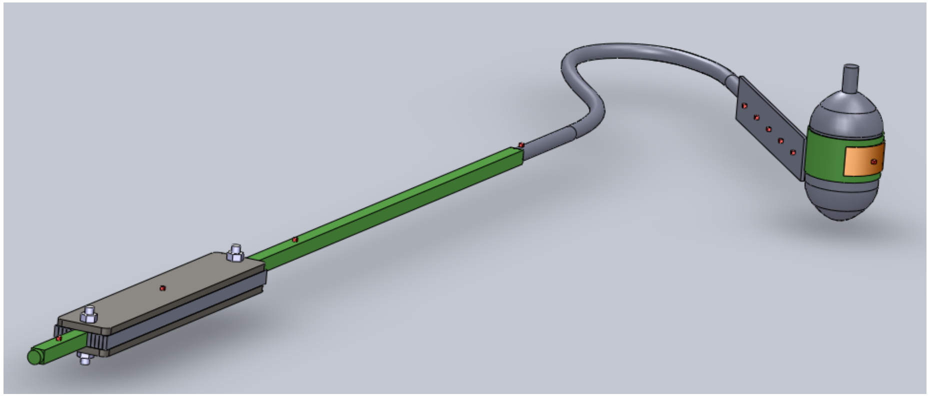

Figure 5. Variable conductance heat pipe showing the placement of the thermocouples (red), Kapton patch heater (gold) and the strip heaters (grey).

section, five on the condenser section and one on each heater. Figure 6 illustrates the dimensions of the heat pipe as well as the measured locations of the thermocouples. The dimensions below the heat pipe represent the length of the

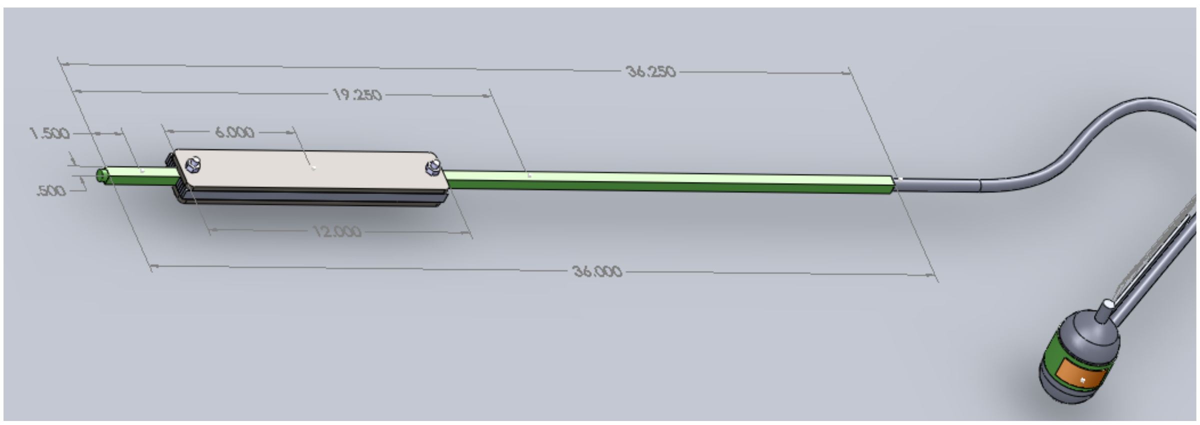

Figure 5. Dimensions of the evaporator section, strip heaters and placement of the thermocouples.

evaporator section, the length of the strip heaters and the diameter of the heat pipe. The dimensions above the heat pipe represent the placement of each thermocouple. Figure 7 displays the dimensions of the condenser section as

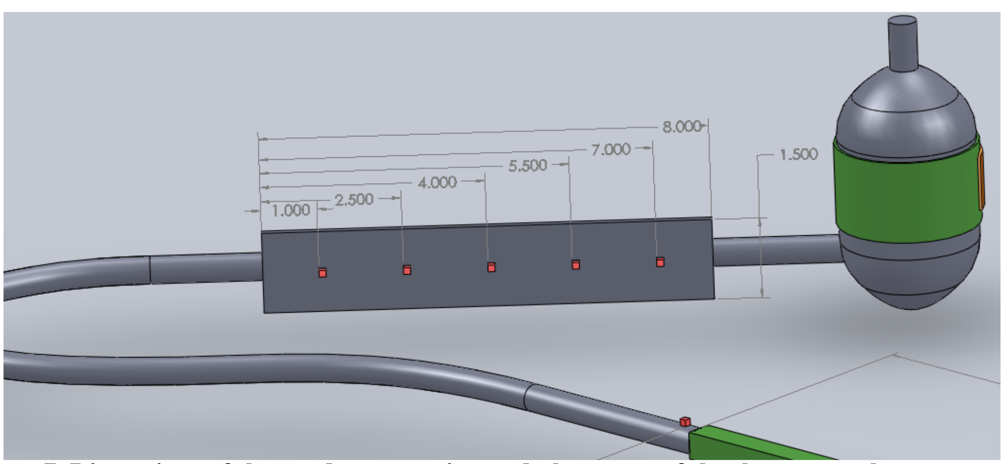

Figure 7. Dimensions of the condensor section and placement of the thermocouples.

well as the placement of the thermocouples. As can be seen in the figure, five thermocouples were used in this section in order to get a better temperature profile and determine if the condenser was open or partially open.

The thermocouples in the evaporator and adiabatic sections determined when “burn-out”, a capillary limitation that allows the evaporator to dry out, was occurring while the thermocouples in the condenser section determined how much of the condenser was open. The thermocouple leads were connected to an 8-port NI USB-6210 National Instruments data acquisition (DAQ) card to translate the thermocouple voltage readings into usable temperatures. The wall temperatures were then sent to a computer equipped with LabView where temperature profiles were plotted. Figure 8 shows the wall temperatures of the heat pipe as seen on LabView and provided real-time profiles in order to determine “burn-out” conditions. The LabView temperatures follow the thermocouple placement on the heat pipe starting with the left thermometer being the thermocouple to the left of the strip heaters and the last five thermometers being the thermocouples on the condenser. The remaining thermocouples were connected to a thermometer and manually read and recorded because the DAQ could only support 8 thermocouples.

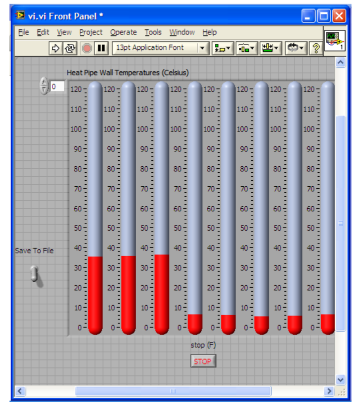

Figure 8. Temperature profile on LabView.

Introducing heat into the evaporator section required heaters, power supplies and accurate measurements. Two S-1202 Chromalox strip heaters were attached to the evaporator section and were powered by two type 116B Powerstat Variable Transformers with a capability of 140 Volts each. The resistance of each strip heater was first measured with a Cen-Tech P35017 multimeter in order to calculate the correct voltage settings for the desired powers. The same multimeter was used during the experiment to verify the correct voltage setting on each Variac.

As shown in Fig. 9, the entire heat pipe, heaters and cooling box were wrapped with foil-backed fiberglass pipe wrap insulation manufactured by Frost King in order to minimize heat losses. This insulation worked very well and was chosen over rubber or polyethylene pipe insulation because it was easy to work with, provided an equivalent R value of 3.3 $h\cdot ft^2\cdot °F/Btu$[3] and could withstand higher temperatures from direct contact with the heaters. The entire heat pipe was wrapped twice giving an R-value of 6.6 $h\cdot ft^2\cdot °F/Btu$ or 1.623 $K\text{-}m^2/W$ when converted to the necessary units. Figure 10 illustrates the placement of the thermocouples on the inner and outer wall of the insulation in order to calculate the losses. A thermocouple was attached to the top heater in order to determine

Figure 9. The VCHP wrapped in foil-backed fiberglass insulation.

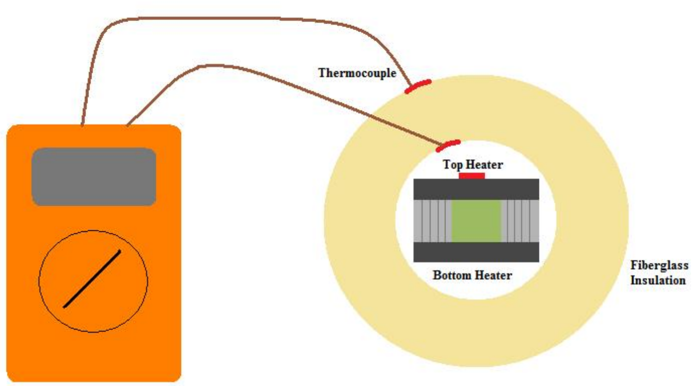

Figure 10. Cross-section of the heat pipe, heaters and insulation illustrating the placement of thermocouples.

steady-state conditions. A steady temperature on the strip heater indicated that all the heat was either going into the evaporator or leaving through the insulation. Due to the limited number of thermocouples and thermometers, only the top heater was monitored. The figure also displays the placement of aluminum bars along the heat pipe between the two strip heaters. These bars allowed the heat pipe to receive heat from all four sides and minimized losses. Thermal grease was used between each bar and along the strip heaters to provide a better thermal conduction.
The reservoir was also equipped with a heater but utilized a Kapton patch heater capable of 30 W of power input. The power for the patch heater was provided by Hewlett-Packard 6038A power supply capable of producing up to 200 W. A thermocouple was also attached to the Kapton patch heater in order to determine steady-state conditions.

Removing heat from the heat pipe required a cooling system capable of accurately measuring the temperature and flow of the coolant (water) as well as the length of the condenser section being used. As shown in Fig. 11, the

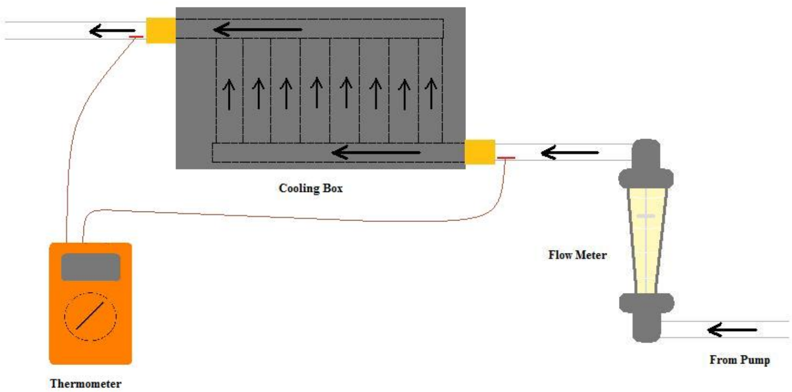

Figure 11. Cooling system set-up.

coolant was fed from a pump, through the flow meter, across a thermocouple, into and out of the cooling box and across another thermocouple. The thermocouples measured the change in water temperature that was needed to calculate the amount of heat removed from the system. The cooling box was machined from 6061 Aluminum and was attached to the heat pipe with C-clamps as shown in Fig. 12. As can be seen in the figure, five thermocouples were placed between the cooling box and the condenser to plot a more accurate temperature profile of the condenser section. Thermal grease was used between the cooling box, condenser and thermocouples in order to minimize thermal resistance.

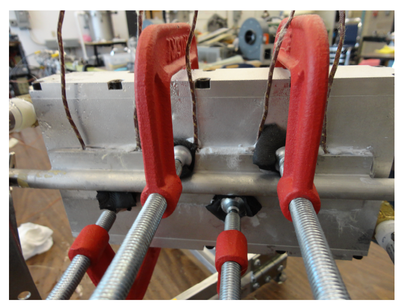

Figure 12. Cooling box attached to the condenser.

Procedure

In order to determine the performance characteristics of the heat pipe, various power inputs as well as inclination angles had to be used. The pipe was first leveled using bubble levelers and allowed to sit for an hour. This allowed any sloshing of the working fluid to be minimal. The heaters, thermocouples, cooling box and hoses were attached and the pipe was then wrapped with insulation. The resistances in the strip heater power sources were measured and the voltages for the various power settings were calculated. A temperature reading was recorded without heat in order to calibrate the thermocouples. The power was then set to 20 W and wall temperatures were recorded once steady-state was reached. Steady-state was realized once the thermocouple attached directly to the strip heater and read by an Omega HH506 Thermometer maintained a temperature to within 1 °C for 20 minutes. A steady temperature reading at the heater indicated that all the heat was entering the pipe or lost through the insulation. Calculating the insulation losses left an accurate measure of the actual heat input at the evaporator. The inclination of the pipe was then raised by 0.25° increments until "burn-out" conditions were reached. This inclination raised the evaporator section above the condenser section and measured the performance of the wick system. If the capillary force of the wick was insufficient to overcome the gravitational force then the liquid could not return to the evaporator causing it to dry out (burn-out).

Figure 13 displays the inclination angle measuring device attached to the test rig. The angles were calculated earlier and markings were placed at 0.25° increments. The heat pipe was again leveled and the process was repeated for 30, 40, 50, 60, 62, 65, 70 and 80 W. The entire process was also repeated using ice-water (3 °C) as a coolant instead of tap water (19 °C) in order to determine the impact on performance. A spacecraft utilizing this heat pipe could undergo various temperature changes which could affect the temperature of the cooling system (radiator) and possibly the performance of the pipe.

The strip heaters at the evaporator were set to a total power of 50 W and the active feedback system was simulated by introducing 1 W of power to the patch heater attached to the reservoir. Once steady-state was reached, the temperatures were recorded and the power to the patch heater was increased by 1 W. This process was repeated until the power reached 8 W upon which burn-out conditions at the evaporator were reached. The decision to use a power setting of 50 W allowed the evaporator to reach burn-out conditions without exceeding the 30 W input power limitation of the Kapton patch heater. The procedure produced temperature profiles reflecting the thermal control of the VCHP with an active feedback system.

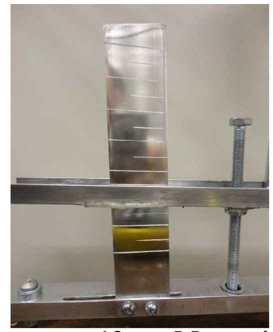

Figure 13. Measuring device on test rig used for inclination angle. Each mark is 0.25 degrees.

III. Analysis

The first step in analyzing the VCHP was to calculate the voltages required from each Variac using the resistances measured for each strip heater and Eq. (1)[4]

$$V = \sqrt{\frac{P}{\frac{1}{R_u}+\frac{1}{R_l}}} \tag{1}$$

where P is the power supplied in watts, R_u is the resistance of the upper strip heater in ohms, R_l is the resistance of the lower strip heater in ohms and V is the voltage needed from each Variac in volts. Voltages were calculated for powers ranging from 10 W to 80 W and measured from each Variac during the experiment for accuracy. Table 1 displays the voltages needed for each power setting, resistances for each strip heater and the total input power.

Table 1. Votages needed from each Variac for each power setting.

Power (W) Both Strip-Heaters	Voltage (V)	Resistance (Ω) Upper Strip-Heater	Resistance (Ω) Lower Strip-Heater
10	17.102	59	58
20	24.186	59	58
30	29.622	59	58
40	34.204	59	58
50	38.241	59	58
60	41.891	59	58
62	42.584	59	58
65	43.602	59	58
70	45.248	59	58
80	48.372	59	58

The input power is the heat flow going into the heat pipe, Q_{in}, at the evaporator and was calculated by subtracting the heat lost, Q_{ins}, through the insulation from the total power supplied.

$$Q_{in} = Q_{sup} - Q_{ins} \tag{2}$$

The power supplied is shown in Eq. (2) as Q_{sup} in order to represent heat flow and P in Eq. (1) to represent energy and are both in watts.

Equation (3)[5] was used to calculate the heat loss through the insulation

$$Q_{ins} = \frac{(T_{in} - T_{out})A}{R} \tag{3}$$

where T_{in} is the insulation inside wall temperature in K, T_{out} is the insulation outside wall temperature in K, A is the outer area of the insulation in m^2 and R is the thermal resistance of the insulation in $K*m^2/W$. Calculating the losses through the insulation allowed for a more accurate performance analysis of the heat pipe.

The amount of heat transported was determined by using Eq. (4)[2]

$$Q_{out} = \dot{m} c_p (T_h - T_c) \tag{4}$$

where Q_{out} is the heat flow out of the condenser in watts, $\dot{m}$ is the mass flow rate of the coolant in kg/s, c_p is the specific heat of water in j/kg*°C, T_h is the temperature of the water leaving the cooling box in K and T_c is the temperature of the water entering the cooling box in K. The change in temperature remains the same whether it is in K or °C allowing it to cancel out with the temperature in the specific heat term.

The difference between the heat flowing in and the heat flowing out in Eq. (5) gave the heat losses along the adiabatic section.

$$Q_{loss} = Q_{in} - Q_{out} \tag{5}$$

This was the longest section of the pipe and accounted for the largest losses.

The radial heat flux, q_r in W/in^2, was calculated using

$$q_r = \frac{Q_{in}}{A} \tag{6}$$

where A is the surface area of the evaporator section being used in in^2.

IV. Results

The various performance trends of the VCHP were found through data collected from thermocouples and temperature profiles. Figure 14 illustrates these heat pipe wall temperature profiles for various evaporator input powers. Thermocouple positions 1 and 2 were found before and after the strip heaters on the evaporator section, position 3 was in the adiabatic section and positions 4-8 were on the condenser section. The heat pipe was found to

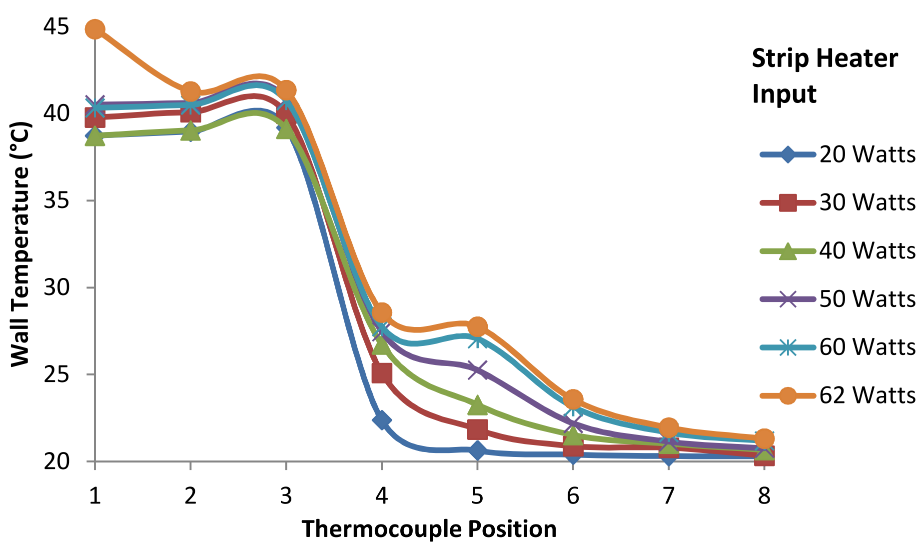

Figure 14. Temperature profiles along heat pipe wall for various input powers.

transfer heat successfully with input powers up to 60 W as shown by the minimal temperature differences between positions 1-3. Burnout was realized once the temperature gradient between positions 1, 2 and 3 grew larger which occurred when the input power was increased to 62 W. Burnout conditions are due to a combination of heat transfer limitations such as capillary limit, sonic limit, boiling limit, entrainment limit and vapor pressure limit which all lead up to a drying out of the evaporator. Figure 14 also illustrates the amount of condenser section being used for each case. Note that positions 7 and 8 never got as hot as the other condenser positions which led to the realization that the cooling system was removing too much heat. Increasing the number of strip heaters on the evaporator section and/or decreasing the flow of coolant through the cooling system could have opened up the condenser section further.

Figure 15 displays another performance trend found during the experiment. Increasing the input power led to a decrease in the necessary inclination angle for burnout conditions to occur. At 20 W input power the heat pipe had to be inclined 2° for the evaporator section to dry out yet at 60 W input power the heat pipe could only withstand an inclination angle of 1°. This led to the conclusion that increasing the radial heat flux caused the vapor to be produced at a faster rate which in turn required more liquid to return to the evaporator and since the wick could not keep up, the trend was probably due to the capillary limitation of the heat pipe.

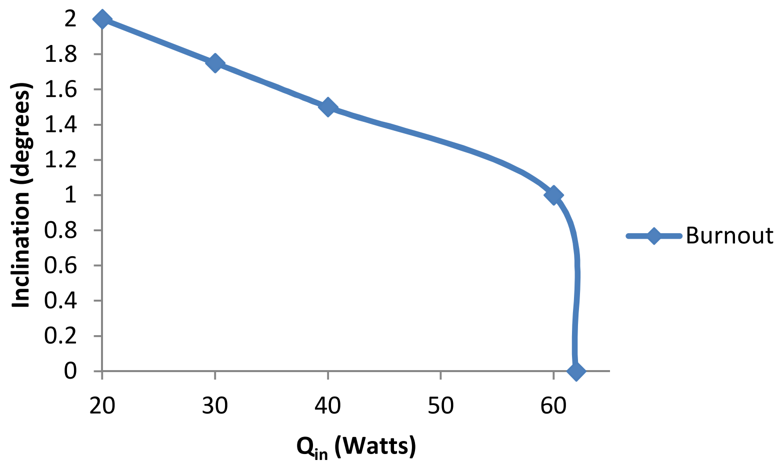

Figure 15. Inclination angle causing Burnout as a function of the input power.

Figure 16 displays the temperature profiles of the heat pipe during burnout conditions. The profiles for input powers between 20W and 60W occurred at various inclination angles as previously explained while the profiles for

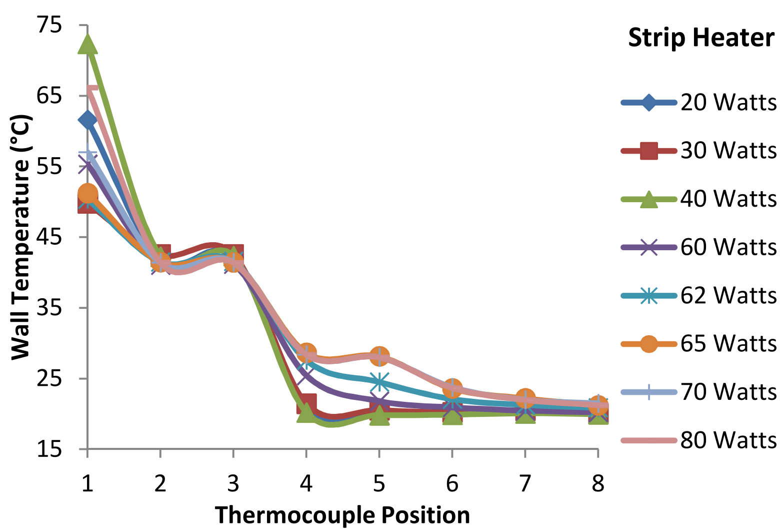

Figure 16. Temperature profiles for the burnout cases.

input powers at 62W and larger occurred with the heat pipe in the horizontal position. At these larger axial heat fluxes, the heat pipe never reached steady-state and the temperature of the thermocouple at position 1 kept rising. Figure 16 is shown in order to illustrate the large temperature gradients between positions 1-3 indicating burnout conditions.

In order to thoroughly investigate the performance of the heat pipe, the coolant was changed from tap water to ice water which brought the temperature of the coolant down from 19 °C to 3 °C. Figure 17 illustrates the heat pipe

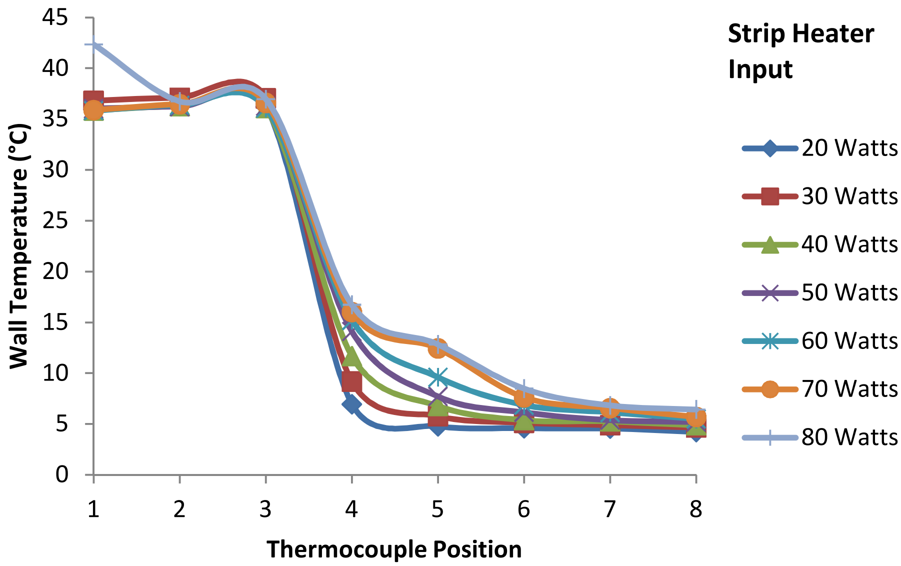

Figure 17. Temperature profiles using ice-water as the coolant.

wall temperature profiles with the ice-water coolant. As can be seen in the figure, the heat pipe reached burnout at a larger radial heat flux of 80 W and had a much cooler wall temperature profile. The evaporator was able to avoid drying out due to the cooler coolant but as can be seen in Fig. 18, the overall performance remained the same. The figure displays the heat transported using the two coolants. The small differences shown in the figure are due to a

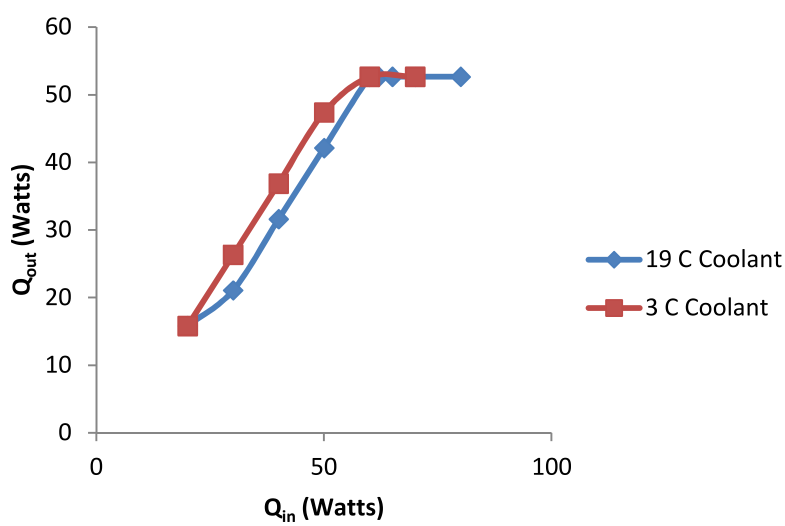

Figure 18. Comparison of the heat transported using two different temperature coolants.

0.1 °C variation in the ΔT of the coolant at the cooling box. Because the coolant flow was so large, small variations in temperature at the cooling box caused a change in Q_{out} but the heat pipe performance remained similar. It was concluded that the heat pipe reached an input power of 80 W before burnout with the ice-water coolant due to the colder working fluid reaching the evaporator and requiring more heat to undergo the phase change from liquid to vapor.

The temperature profiles and data shown had been taken using a passive VCHP system but in order to find the type of control a VCHP can provide, an active feedback system was analyzed. By attaching a small patch heater to the non-condensable gas reservoir, the active portion of the condenser could be controlled therefore controlling the temperature at the evaporator section. Figure 19 displays the type of temperature control the VCHP with an active

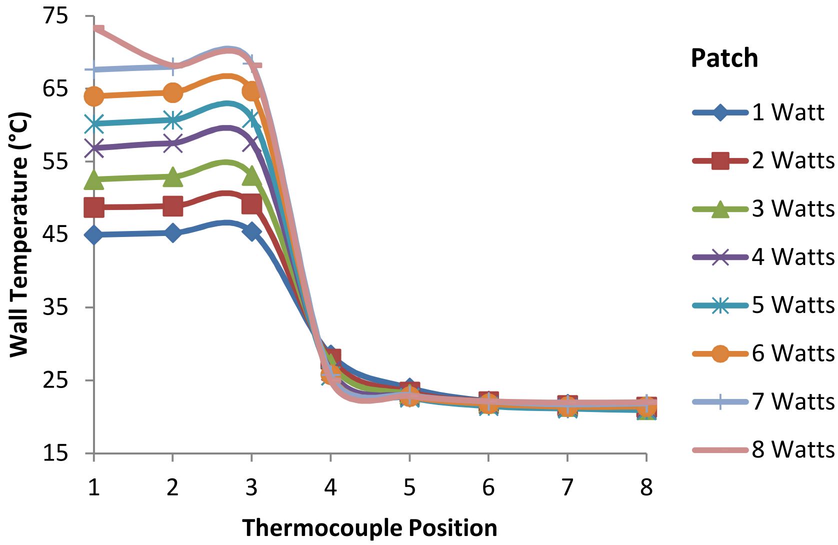

Figure 19. Temperature profile of a VCHP with an active feedback system.

feedback system had. The input power at the evaporator was maintained at 50 W while the patch heater attached to the reservoir was increased from 1W to 8W. As can be seen in the figure, the temperature at the evaporator was controlled between 45 °C to 68 °C. At 8W input power, the evaporator reached burnout conditions. For each Watt increase at the reservoir, there was a 4 °C increase at the evaporator allowing for precise temperature control of any component attached to the heat pipe.

It is important to note that the input powers in Figs. 14-19 are the powers set at the Variacs and do not include the heat losses through the insulation. The actual heat inputs to the VCHP are shown in Table 2. The table displays the data collected and calculated for the passive VCHP system for both coolants. As can be seen on the table, the Q supplied to the strip heaters was not the same as the Q into the heat pipe. The losses through the insulation were first calculated and subtracted from the Q supplied. The last two rows in the table

Table 2. Data collected for the passive VCHP system.

Ice Water Coolant									
Room-Temperature Water Coolant									
$Q_{supplied}$ Strip Heaters (W)	20	30	40	50	60	62	65	70	80
Strip Heater Temp (°C)	37.8	39.9	40.3	41.5	42.8			44.7	
	41.2	42.3	43.9	45.9	48.4	48.5	51.4	58.2	72.8
$T_{insulation}$ Inside (°C)	33.3	34.4	34.6	35.4	36.2			37.6	
	36.2	36.4	38	38.8	40.7	40.5	41.9	44.7	52.4
$T_{insulation}$ Outside (°C)	25.7	25.8	26.2	26.5	26.9			27.6	
	27.5	26.6	28.2	27.6	29.2	28.7	29.7	31.1	34.6
$\Delta T_{insulation}$ (°C or K)	7.6	8.6	8.4	8.9	9.3			10	
	8.7	9.8	9.8	11.2	11.5	11.8	12.2	13.6	17.8
R Value of Insulation (K-m^2/W)	1.1623	1.1623	1.1623	1.1623	1.1623			1.1623	
	1.1623	1.1623	1.1623	1.1623	1.1623	1.1623	1.1623	1.1623	1.1623
Area of Insulation (m^2)	0.0973	0.0973	0.0973	0.0973	0.0973			0.0973	
	0.0973	0.0973	0.0973	0.0973	0.0973	0.0973	0.0973	0.0973	0.0973
$Q_{insulation}$ (W)	0.6361	0.7198	0.7031	0.7449	0.7784			0.837	
	0.7282	0.8203	0.8203	0.9375	0.9626	0.9877	1.0212	1.1383	1.4899
Q_{in} (W)	19.364	29.28	39.297	49.255	59.222			69.163	
	19.272	29.18	39.18	49.063	59.037	61.012	63.979	68.862	78.51

represent the actual Wattage input to the heat pipe. For example, the maximum radial heat input before reaching burnout conditions was 60 W and the heat lost through the insulation was 0.9626 W leaving 59.037 W of actual heat going into the evaporator. The same method of calculating the heat input was utilized for the active feedback system as shown in Table 3. For this part of the experiment the power to the strip heaters was set to 50 W while the power to the patch heater attached to the reservoir was varied from 1-8 W. As the $Q_{insulation}$ row shows, the heat lost through the insulation increased as the patch heater input power was increased. This was due to the increase in temperature at the evaporator caused by the closing of the condenser section.

Due to the limited number of strip heaters available for the experiment, the axial heat transport capacity of the VCHP could not be determined, however, the radial heat transport capacity was found to be 2.46 W/in^2. This was calculated by dividing the maximum input power (before burnout), 59.037 W, by the area of the evaporator section being used, 24 in^2.

Table 3. Data collected for the active feedback VCHP system.

	Using Patch Heater							
$Q_{supplied}$ Patch (W)	1	2	3	4	5	6	7	8
$Q_{supplied}$ Strip Heaters (W)	50	50	50	50	50	50	50	50
Strip Heater Temp (°C)	49.5	53.3	57.3	61.7	64.8	68.6	72.2	77.3
$T_{insulation}$ Inside (°C)	41.4	44.1	47.1	50.5	53.1	56	58.7	62.1
$T_{insulation}$ Outside (°C)	28.3	29.7	30.7	32.1	33.3	34.2	35.1	36.8
$\Delta T_{insulation}$ (°C or K)	13.1	14.4	16.4	18.4	19.8	21.8	23.6	25.3
R Value of Insulation (K-m^2/W)	1.1623	1.1623	1.1623	1.1623	1.1623	1.1623	1.1623	1.1623
Area of Insulation (m^2)	0.0973	0.0973	0.0973	0.0973	0.0973	0.0973	0.0973	0.0973
$Q_{insulation}$ (W)	1.0965	1.2053	1.3727	1.5401	1.6573	1.8247	1.9753	2.1176
Q_{in} (W)	48.904	48.795	48.627	48.46	48.343	48.175	48.025	47.882

V. Conclusion

The performance analysis of a VCHP is an important step in development in order to verify performance claims, verify design calculations or maintain quality control. A simple analysis of the wall temperatures can lead to performance trends without knowing the wick structure or inner workings of the heat pipe and could offer support for the design predictions or unveil poor heat transport capabilities. The performance analysis found that the passive VCHP was great for controlling heat and the active feedback VCHP was truly amazing with its precise temperature control capabilities and both were found through temperature profiles.

The experiment presented challenges such as avoiding heat losses and designing the heating and cooling systems. Although a good insulator was used on the experiment and the wrapping was thought to be sufficient, there was a portion of the adiabatic section where some heat loss was noticed. Also, the accuracy of the measurements at the cooling box suffered due to the fact that the minimum coolant flow was 0.2 GPM. The cooling and heating systems were difficult to design without having some idea of the heat transport capability of the VCHP. Obtaining more heaters for the experiment could have led to more performance data (axial heat transport capability).

There are still areas of interest and possible experiments with this VCHP. Increasing the number of strip heaters on the evaporator could result in the axial heat transport capability being found, using a less efficient cooling system could allow the condenser section to be fully opened and the relationship between the temperature of the coolant and the radial heat transport capability could be looked into further. In this experiment the coolant temperature was decreased by 16 °C and it led to an increase in burnout temperature at the evaporator by about the same amount. Various coolant temperatures could be used to find this relationship.

References

[1]Dunn, P. D., and D. A. Reay. *Heat Pipes*. 4th ed. Oxford, England: Pergamon, 1994. Print.

[2]Faghri, Amir. *Heat Pipe Science and Technology*. Washington, DC: Taylor & Francis, 1995. Print.

[3]*Frost King*. Web. 17 Nov. 2011. <http://www.frostking.com/>.

[4]Alexander, Charles K., and Matthew N. O. Sadiku. *Fundamentals of Electric Circuits*. 2nd ed. Boston, Mass. [u.a.: McGraw-Hill, 2004. Print.

[5]Holman, J. P. *Heat Transfer*. 10th ed. Boston: McGraw-Hill Higher Education, 2010. Print.

Raw Data

Steady-State Using Tap Water

20 Watts								
Location	**1**	**2**	**3**	**4**	**5**	**6**	**7**	**8**
Temperature (°C)	38.7269	38.9630568	39.19054	22.38379	20.63976	20.40089	20.31958	20.30996
30 Watts								
Location	**1**	**2**	**3**	**4**	**5**	**6**	**7**	**8**
Temperature (°C)	39.77466	40.07508194	39.98826	25.08552	21.84281	20.88133	20.79024	20.33291
40 Watts								
Location	**1**	**2**	**3**	**4**	**5**	**6**	**7**	**8**
Temperature (°C)	38.73013	39.03238434	39.12444	26.73082	23.2623	21.52066	21.02637	20.66421
50 Watts								
Location	**1**	**2**	**3**	**4**	**5**	**6**	**7**	**8**
Temperature (°C)	40.50925	40.60974826	40.82566	27.46606	25.26147	22.1972	21.15094	20.76751
60 Watts								
Location	**1**	**2**	**3**	**4**	**5**	**6**	**7**	**8**
Temperature (°C)	40.32725	40.49224372	40.73877	27.74967	27.05813	23.14504	21.66717	21.18722
62 Watts								
Location	**1**	**2**	**3**	**4**	**5**	**6**	**7**	**8**
Temperature (°C)	44.85229	41.27295041	41.35034	28.5673	27.75409	23.57859	21.95547	21.31832

Steady-State Using Ice-Water Coolant

20 Watts								
Location	**1**	**2**	**3**	**4**	**5**	**6**	**7**	**8**
Temperature (°C)	35.92971	36.2909	36.21033	6.95188	4.774172	4.576189	4.538854	4.214735
30 Watts								
Location	**1**	**2**	**3**	**4**	**5**	**6**	**7**	**8**
Temperature (°C)	36.80243	37.09225	37.03919	9.180559	5.773592	5.117307	4.879744	4.659896
40 Watts								
Location	**1**	**2**	**3**	**4**	**5**	**6**	**7**	**8**
Temperature (°C)	35.84242	36.26837	36.07452	11.68614	6.782719	5.387019	5.263648	4.888268
50 Watts								
Location	**1**	**2**	**3**	**4**	**5**	**6**	**7**	**8**
Temperature (°C)	36.02832	36.22303	36.26523	14.10257	7.720425	6.166266	5.389391	5.209276
60 Watts								
Location	**1**	**2**	**3**	**4**	**5**	**6**	**7**	**8**
Temperature (°C)	35.82463	36.36205	36.07932	15.20147	9.594887	6.856071	6.137217	5.497179
70 Watts								
Location	**1**	**2**	**3**	**4**	**5**	**6**	**7**	**8**
Temperature (°C)	35.87956	36.45422	36.5836	16.0082	12.43819	7.621819	6.559047	5.694065
80 Watts								
Location	**1**	**2**	**3**	**4**	**5**	**6**	**7**	**8**
Temperature (°C)	42.34333	36.73534	36.96819	16.73553	12.83418	8.489826	6.83366	6.436899

Burn-Out

20 Watts								
Location	**1**	**2**	**3**	**4**	**5**	**6**	**7**	**8**
Temperature (°C)	61.59524	41.90365	42.13378	20.70579	20.15258	20.07277	20.2474	20.06387
Inclination (deg)	2							
30 Watts								
Location	**1**	**2**	**3**	**4**	**5**	**6**	**7**	**8**
Temperature (°C)	49.76897	42.53714	42.56302	21.44181	20.51672	20.22691	20.45403	20.06221
Inclination (deg)	1.75							
40 Watts								
Location	**1**	**2**	**3**	**4**	**5**	**6**	**7**	**8**
Temperature (°C)	72.34594	42.22209	42.32674	20.20062	19.81453	19.86767	20.06692	19.94575
Inclination (deg)	1.5							
60 Watts								
Location	**1**	**2**	**3**	**4**	**5**	**6**	**7**	**8**
Temperature (°C)	55.31304	41.04604	41.16849	25.43337	21.80017	20.91248	20.45734	20.21314
Inclination (deg)	1							
62 Watts								
Location	**1**	**2**	**3**	**4**	**5**	**6**	**7**	**8**
Temperature (°C)	50.36357	41.49184	41.59332	27.59809	24.51488	22.10219	21.27223	20.87411
Inclination (deg)	0							
65 Watts								
Location	**1**	**2**	**3**	**4**	**5**	**6**	**7**	**8**
Temperature (°C)	51.21827	41.46444	41.43886	28.65355	28.15483	23.59655	22.21752	21.19706
Inclination (deg)	0							
70 Watts								
Location	**1**	**2**	**3**	**4**	**5**	**6**	**7**	**8**
Temperature (°C)	57.02346	41.41619	41.45172	28.39307	28.00338	23.78464	22.01119	21.50844
Inclination (deg)	0							
80 Watts								
Location	**1**	**2**	**3**	**4**	**5**	**6**	**7**	**8**
Temperature (°C)	66.1529	41.37918	41.36001	28.35233	27.98382	23.65217	21.96205	21.21507
Inclination (deg)	0							

Active Feedback System-Patch Heater @ 50 Watt Strip Heaters								
1 Watt								
Location	**1**	**2**	**3**	**4**	**5**	**6**	**7**	**8**
Temperature (°C)	44.95978	45.23483	45.41462	28.51034	23.96885	22.18082	21.76548	21.24461
2 Watts								
Location	**1**	**2**	**3**	**4**	**5**	**6**	**7**	**8**
Temperature (°C)	48.71988	48.90136	49.19739	27.93704	23.39643	22.10056	21.5672	21.34621
3 Watts								
Location	**1**	**2**	**3**	**4**	**5**	**6**	**7**	**8**
Temperature (°C)	52.54816	52.94778	53.11704	27.30147	23.11828	21.85155	21.4099	20.99214
4 Watts								
Location	**1**	**2**	**3**	**4**	**5**	**6**	**7**	**8**
Temperature (°C)	56.85471	57.52553	57.66412	26.2985	22.83023	21.66971	21.31976	21.12492
5 Watts								
Location	**1**	**2**	**3**	**4**	**5**	**6**	**7**	**8**
Temperature (°C)	60.16503	60.69342	60.96053	25.61792	22.6207	21.44854	21.12142	20.89212
6 Watts								
Location	**1**	**2**	**3**	**4**	**5**	**6**	**7**	**8**
Temperature (°C)	63.95662	64.46211	64.6749	25.78609	22.78438	21.79916	21.40495	21.40355
7 Watts								
Location	**1**	**2**	**3**	**4**	**5**	**6**	**7**	**8**
Temperature (°C)	67.63438	68.02364	68.4551	25.74033	22.989	22.10546	21.70486	21.8411
8 Watts								
Location	**1**	**2**	**3**	**4**	**5**	**6**	**7**	**8**
Temperature (°C)	73.36813	68.16953	68.21093	25.02183	22.84825	22.12511	21.97844	22.02453

Room-Temperature Water Coolant

$Q_{supplied}$ Strip Heaters (W)	**20**	**30**	**40**	**50**	**60**	**62**	**65**	**70**	**80**
Strip Heater Temp (°C)	41.2	42.3	43.9	45.9	48.4	48.5	51.4	58.2	72.8
$T_{insulation}$ Inside (°C)	36.2	36.4	38	38.8	40.7	40.5	41.9	44.7	52.4
$T_{insulation}$ Outside (°C)	27.5	26.6	28.2	27.6	29.2	28.7	29.7	31.1	34.6
$\Delta T_{insulation}$ (°C or K)	8.7	9.8	9.8	11.2	11.5	11.8	12.2	13.6	17.8
R Value of Insulation (K-m^2/W)	1.162326	1.162326	1.162326	1.162326	1.162326	1.162326	1.162326	1.162326	1.162326
Area of Insulation (m^2)	0.09728793	0.097288	0.097288	0.097288	0.097288	0.097288	0.097288	0.097288	0.097288
$Q_{insulation}$ (W)	0.728199311	0.82027	0.82027	0.937452	0.962562	0.987673	1.021153	1.138335	1.489879
Q_{in} (W)	19.27180069	29.17973	39.17973	49.06255	59.03744	61.01233	63.97885	68.86167	78.51012
Water Inlet (°C)	19.6	19	19.9	18.8	19.7	19.1	19.2	19.4	19.4
Water Outlet (°C)	19.9	19.4	20.5	19.6	20.7	20.1	20.2	20.4	20.4
ΔT_{water} (°C or K)	0.3	0.4	0.6	0.8	1	1	1	1	1
Water Flow (kg/s)	0.0125972	0.012597	0.012597	0.012597	0.012597	0.012597	0.012597	0.012597	0.012597
C_p water j/kg*°C	4179	4179	4179	4179	4179	4179	4179	4179	4179
Q_{out}	15.79310964	21.05748	31.58622	42.11496	52.6437	52.6437	52.6437	52.6437	52.6437

Ice Water Coolant

$Q_{supplied}$ Strip Heaters (W)	**20**	**30**	**40**	**50**	**60**	**70**
Strip Heater Temp (°C)	37.8	39.9	40.3	41.5	42.8	44.7
$T_{insulation}$ Inside (°C)	33.3	34.4	34.6	35.4	36.2	37.6
$T_{insulation}$ Outside (°C)	25.7	25.8	26.2	26.5	26.9	27.6
$\Delta T_{insulation}$ (°C or K)	7.6	8.6	8.4	8.9	9.3	10
R Value of Insulation (K-m^2/W)	1.162326	1.162326	1.162326	1.162326	1.162326	1.162326
Area of Insulation (m^2)	0.097288	0.097288	0.097288	0.097288	0.097288	0.097288
$Q_{insulation}$ (W)	0.636128	0.719829	0.703089	0.74494	0.77842	0.837011
Q_{in} (W)	19.36387	29.28017	39.29691	49.25506	59.22158	69.16299
Water Inlet (°C)	2.6	2.7	2.6	2.7	3	3.4
Water Outlet (°C)	2.9	3.2	3.3	3.6	4	4.4
ΔT_{water} (°C or K)	0.3	0.5	0.7	0.9	1	1
Water Flow (kg/s)	0.012597	0.012597	0.012597	0.012597	0.012597	0.012597
C_p water j/kg*°C	4179	4179	4179	4179	4179	4179
Q_{out}	15.79311	26.32185	36.85059	47.37933	52.6437	52.6437

Using Patch Heater								
$Q_{supplied}$ Patch (W)	**1**	**2**	**3**	**4**	**5**	**6**	**7**	**8**
$Q_{supplied}$ Strip Heaters (W)	**50**	**50**	**50**	**50**	**50**	**50**	**50**	**50**
Strip Heater Temp (°C)	49.5	53.3	57.3	61.7	64.8	68.6	72.2	77.3
$T_{insulation}$ Inside (°C)	41.4	44.1	47.1	50.5	53.1	56	58.7	62.1
$T_{insulation}$ Outside (°C)	28.3	29.7	30.7	32.1	33.3	34.2	35.1	36.8
$\Delta T_{insulation}$ (°C or K)	13.1	14.4	16.4	18.4	19.8	21.8	23.6	25.3
R Value of Insulation (K-m^2/W)	1.162326	1.162326	1.162326	1.162326	1.162326	1.162326	1.162326	1.162326
Area of Insulation (m^2)	0.097288	0.097288	0.097288	0.097288	0.097288	0.097288	0.097288	0.097288
$Q_{insulation}$ (W)	1.096484	1.205295	1.372698	1.5401	1.657281	1.824683	1.975345	2.117637
Q_{in} (W)	48.90352	48.7947	48.6273	48.4599	48.34272	48.17532	48.02465	47.88236
Water Inlet (°C)	18.5	18.6	18.5	18.5	18.2	18.6	19	19.2
Water Outlet (°C)	19.4	19.3	19.2	19.2	18.8	19.1	19.6	19.8
ΔT_{water} (°C or K)	0.9	0.7	0.7	0.7	0.6	0.5	0.6	0.6
Water Flow (kg/s)	0.012597	0.012597	0.012597	0.012597	0.012597	0.012597	0.012597	0.012597
C_p water j/kg*°C	4179	4179	4179	4179	4179	4179	4179	4179
Q_{out}	47.37933	36.85059	36.85059	36.85059	31.58622	26.32185	31.58622	31.58622
Patch Heater Temp (°C)	25.3	31.2	36.9	43.5	48	53.1	57.8	63
$T_{insulation}$ Outside (°C)	20.4	21.9	23.5	25.1	26.3	27.9	29.1	30.3
$\Delta T_{insulation}$ (°C or K)	4.9	9.3	13.4	18.4	21.7	25.2	28.7	32.7
R Value of Insulation (K-m^2/W)	1.162326	1.162326	1.162326	1.162326	1.162326	1.162326	1.162326	1.162326
Area of Insulation (m^2)	0.020268	0.020268	0.020268	0.020268	0.020268	0.020268	0.020268	0.020268
$Q_{insulation}$ (W)	0.085445	0.162171	0.233665	0.320854	0.378399	0.439431	0.500463	0.570214
Q_{in} (W)	0.914555	1.837829	2.766335	3.679146	4.621601	5.560569	6.499537	7.429786